Green's function multiple-scattering theory with a truncated basis set: An augmented-KKR formalism

Aftab Alam,[1,*] Suffian N. Khan,[2] A. V. Smirnov,[2] D. M. Nicholson,[3,†] and Duane D. Johnson[2,4,‡]

[1]*Department of Physics, Indian Institute of Technology, Bombay, Powai, Mumbai 400 076, India*

[2]*Division of Materials Science & Engineering, Ames Laboratory, Ames, Iowa 50011, USA*

[3]*Oak Ridge National Laboratory, Oak Ridge, Tennessee 37831, USA*

[4]*Department of Materials Science & Engineering, Iowa State University, Ames, Iowa 50011, USA*

(Received 16 August 2014; revised manuscript received 6 October 2014; published 4 November 2014)

The Korringa-Kohn-Rostoker (KKR) Green's function, multiple-scattering theory is an efficient site-centered, electronic-structure technique for addressing an assembly of N scatterers. Wave functions are expanded in a spherical-wave basis on each scattering center and indexed up to a maximum orbital and azimuthal number $L_{\max} = (l,m)_{\max}$, while scattering matrices, which determine spectral properties, are truncated at $L_{tr} = (l,m)_{tr}$ where phase shifts $\delta_{l>l_{tr}}$ are negligible. Historically, $L_{\max}$ is set equal to L_{tr}, which is correct for large enough $L_{\max}$ but not computationally expedient; a better procedure retains higher-order (free-electron and single-site) contributions for $L_{\max} > L_{tr}$ with $\delta_{l>l_{tr}}$ set to zero [X.-G. Zhang and W. H. Butler, Phys. Rev. B **46**, 7433 (1992)]. We present a numerically efficient and accurate *augmented*-KKR Green's function formalism that solves the KKR equations by exact matrix inversion [$\mathcal{R}^3$ process with rank $N(l_{tr}+1)^2$] and includes higher-L contributions via linear algebra [$\mathcal{R}^2$ process with rank $N(l_{\max}+1)^2$]. The augmented-KKR approach yields properly normalized wave functions, numerically cheaper basis-set convergence, and a total charge density and electron count that agrees with Lloyd's formula. We apply our formalism to fcc Cu, bcc Fe, and $L1_0$ CoPt and present the numerical results for accuracy and for the convergence of the total energies, Fermi energies, and magnetic moments versus $L_{\max}$ for a given L_{tr}.

DOI: 10.1103/PhysRevB.90.205102 PACS number(s): 71.15.Ap, 71.15.Dx, 61.50.−f

I. INTRODUCTION

Multiple-scattering theory, as formulated by Korringa [1], Kohn, and Rostoker [2] (KKR), continues to be a powerful and efficient method to study the electronic structure of solids [3]. KKR theory is Rayleigh-Ritz variational, like the related muffin-tin orbital (MTO) and augmented plane-wave (APW) methods. KKR Green's function (GF) techniques have facilitated numerous successful applications to spectral and energy-related properties, such as surfaces [3], alloys [4–7], interfaces [8,9], quantum criticality [10], and transport [11]. Due to its inherent multiple-scattering nature, KKR GF techniques are used extensively to predict and analyze experimental results [12] involving low-energy electron diffraction (LEED) [13,14], photoemission [15–17], and neutron and x-ray scattering [18–20].

A key parameter controlling KKR convergence is the maximum orbital and azimuthal number $L_{\max} = (l,m)_{\max}$ of the truncated spherical-wave basis on each scattering center. Historically, at a wave vector $\mathbf{k}$ and energy E, $L_{\max}$ was also chosen to control truncation of the single-site scattering $t_{LL'}(E)$ matrices and KKR scattering-path operator $\tau_{LL'}(\mathbf{k};E)$ that dictates spectral properties of the system. However, $\tau_{LL'}(\mathbf{k};E)$, i.e., the Green's function (G), could be truncated at $L_{tr} < L_{\max}$, where phase shifts $\delta_{l>l_{tr}}$ are negligible (set to zero), giving smaller matrices to invert if we could directly include the contribution of higher L's ($L_{\max} > L_{tr}$) via the single-site and free-electron part of G.

All electronic-structure methods based on density functional theory (DFT) involve numerous approximations from, e.g., exchange correlation, pseudopotentials, and shape of potential. For multiple-scattering theory, L truncation yields an inherent error often ignored because of the rapid rise in computational cost with $L_{\max}$. In addition, the errors arising from L truncation often are handled in an uncontrollable fashion. For L_{tr} equal to $L_{\max}$, researchers find *apparent* convergence in close-packed systems using $l_{\max} \sim 3$. Yet, a key source of error is due to the normalization of wave functions (Ψ), affecting the charge density $\rho(\mathbf{r})$ and density of states (DOS) $n(E)$ calculated from the Green's functions. As such, if Ψ is not correctly normalized, the integrated DOS from the L_{tr}-truncated basis does not exactly reproduce the total number of electrons in the system, and the Fermi energy E_{F} is slightly incorrect—a possible issue in systems with spectral gaps. Also, L truncation introduces error in the dipole matrix elements, which couple l and $l \pm 1$ states, needed for calculations of transport, electron-phonon, and atomic forces.

So, a balance is struck between convergence of KKR GF properties versus $l_{\max}$ and numerical efficiency for inverting KKR matrices with rank $N(l_{\max}+1)^2$. Butler [21] investigated the accuracy and convergence of multiple-scattering theory versus l for two muffin-tin scatterers in a two-center expansion, showing a solution can be made arbitrarily accurate at some numerically costly $l_{\max} \to 60$. Zhang and Butler [22] established a more proper procedure: Solve the secular equation to L_{tr} and retain $L_{\max} > L_{tr}$ contributions with $\delta_{l>l_{tr}}$ set to zero, yielding continuous and correctly normalized wave functions and an electron count from the DOS that agreed with that from Lloyd's formula. This formalism was derived

*aftab@phy.iitb.ac.in

†Present address: Department of Physics, University of North Carolina Asheville, Asheville, NC 28804.

‡ddj@ameslab.gov

in real space but never implemented for realistic materials. No equivalent KKR GF in reciprocal space was derived or tested.

We present an augmented-KKR GF formulation that yields normalized wave functions, numerically fast basis-set convergence, and an electron count that agrees with Lloyd's formula. Importantly, the augmented KKR formulation agrees well with the standard KKR formulation using exact inversion to $L_{\max}$. We tested convergence of total energy, $E_{\rm F}$ (integrated DOS), and magnetic moments in three systems: fcc Cu, magnetic bcc Fe, and magnetic $L1_0$ CoPt. The efficiency of the augmented KKR formulation arises because the matrices of rank ($\mathcal{R}$) $N(l_{tr}+1)^2$ are solved by direct inversion ($\mathcal{R}^3$ process) and contributions above L_{tr} are included by a closed-form ($\delta_l \to 0$) linear algebra ($\mathcal{R}^2$ process) augmentation of the matrices of rank $N(l_{\max}+1)^2$.

II. FORMALISM

In KKR GF theory, the site-diagonal Green's function at a specific energy E is given by

$$G(\mathbf{r},\mathbf{r}';E) = \sum_{LL'}\big[Z^n_L(\mathbf{r},E)\tau^{nn}_{LL'}(E)Z^n_{L'}(\mathbf{r}',E) - Z^n_L(\mathbf{r}_<,E)\,J^n_{L'}(\mathbf{r}_>,E)\delta_{LL'}\big], \quad (1)$$

where $L=(l,m)$ for the site-centered, spherical-harmonic basis set. Here, $\mathbf{r}_<$ ($\mathbf{r}_>$) denotes one of two vectors $\mathbf{r}$ or $\mathbf{r}'$ with the smaller (larger) absolute value. The tensor $\tau^{nn'}_{LL'}(E)$ is the scattering-path operator [23] describing the propagation pathway of electrons in an array of scattering centers. $Z^n_L(\mathbf{r},E)$ and $J^n_L(\mathbf{r},E)$ are, respectively, the regular and irregular solutions of the Schrödinger equation in the nth Wigner-Seitz cell. $Z^n_L(\mathbf{r},E)$ has the form

$$Z^n_L(\mathbf{r};E) = \kappa\sum_{L'}\phi^n_{L'}(\mathbf{r},E)\big[S^n_{L'L}(E)\big]^{-1}, \quad (2)$$

where $\kappa=\sqrt{E-v_0}$. Here, v_0 is an arbitrary reference energy for an exact theory, but, for approximate cases, such as muffin-tin (MT) or atomic sphere approximations (ASAs), it can be chosen variationally to match the trace of eigenvalues of the exact theory [24]. $\phi^n_{L'}(\mathbf{r},E)$ is the wave-function solution with potential $v_n(\mathbf{r})$, i.e.,

$$[-\nabla^2+v_n(\mathbf{r})]\phi^n_L(\mathbf{r},E) = E\phi^n_L(\mathbf{r},E). \quad (3)$$

The potential vanishes outside the convex cell, so ϕ^n_L joins smoothly to a combination of spherical Bessel $j_l(\kappa r)$ and Neumann $n_l(\kappa r)$ functions beyond the circumscribing sphere (CS) radii around the cell ($r > R_{\rm CS}$), i.e.,

$$\phi^n_L(\mathbf{r},E) = \sum_{L'}\big[n_{l'}(\kappa r)S^n_{L'L}(E) - j_{l'}(\kappa r)C^n_{L'L}(E)\big]Y_{L'}(\widehat{r}). \quad (4)$$

The sine $\mathbf{S}$ and cosine $\mathbf{C}$ matrices are calculated by matching the continuity of the logarithmic derivative of ϕ^n_L across the cell boundary. Notably, $J^n_L(\mathbf{r},E)$ has the asymptotic limit

$$J^n_L(\mathbf{r},E) \to j_l(\kappa r)Y_L(\widehat{r}), \quad r > R_{\rm CS}. \quad (5)$$

A. KKR GF formalism

While constructing $\tau^{ij}_{LL'}(E)$, the propagation of electrons from one scattering center i to another j is defined by the free-electron Green's function $\mathbf{g}^{ij}_{LL'}(E)$ (in a spherical-harmonic basis) or in a solid the KKR structure constant matrix $\mathbf{g}^{nn'}_{LL'}(\mathbf{k};E)$ with basis sites on n,n' sublattices. In a solid, with periodic boundary conditions invoked, $\tau^{nn'}_{LL'}(\mathbf{k};E)$ is given in finite matrix form as

$$\tau = (\mathbf{1}-\mathbf{tg})^{-1}\mathbf{t} = \mathbf{t}+\mathbf{tgt}+\mathbf{tg}\tau\mathbf{gt}, \quad (6)$$

where $\mathbf{t}$ is the single-site scattering matrix, which in a cell n is generally given by

$$\mathbf{t}^n = -\kappa^{-1}(\mathbf{C}^n - i\mathbf{S}^n)^{-1}\mathbf{S}^n. \quad (7)$$

For a spherically symmetric scatterer [25] (used here), the single-site t matrices simplify as

$$t_{LL'}(E) \to t_l(E)\delta_{LL'} = -\kappa^{-1}\sin\delta_l(E)\,e^{i\delta_l(E)}. \quad (8)$$

For MT or ASA scattering centers, the KKR phase shifts are determined by matching the free-electron solution on the sphere boundary.

Generally, the full GF (1) can be rewritten by Eq. (6) in terms of single-site and multiple-scattering pieces, i.e.,

$$\mathbf{G}(\mathbf{r},\mathbf{r}';E) = (\mathbf{ZtZ}-\mathbf{ZJ})+\mathbf{Z}(\tau-\mathbf{t})\mathbf{Z} = (\mathbf{ZtZ}-\mathbf{ZJ})+\mathbf{Zt(g)tZ}+\mathbf{Zt(g}\tau\mathbf{g)tZ}. \quad (9)$$

Each quantity above is a supermatrix in a space of angular momentum [rank $(l+1)^2$] and of unit cell size N, giving a total rank of $\mathcal{R}=N(l+1)^2$.

The three major computational expenditures in KKR GF theory are calculations of (1) structure constants $\mathbf{g}$; (2) wave functions $\mathbf{Z}$ and $\mathbf{J}$; and, most costly, (3) $\boldsymbol{\tau}$ from Eq. (6), which requires an $\mathcal{R}^3$ operation for the inversion. Now, with N fixed, L is usually truncated in numerical calculations to a small but necessary value (e.g., $L=3$), above which the phase shifts δ_l are assumed to be zero, but not an L where the higher-order terms can necessarily be ignored—an error.

B. Augmented-KKR GF

While free-electron contributions remain at all L's, the phase shift δ_l for a spherical scatterer decays rapidly (at standard temperatures and pressures) with increasing value of L. Thus, while the first line of Eq. (9) is convenient numerically (e.g., for pole cancellation and contour integration, and finite-temperature Matsubara sums [26–28]), the second line provides a simple means to account for KKR multiple-scattering solutions exactly the same way as in the conventional KKR GF theory up to L_{tr} and then augmented with single-site and free-electron contributions from $L_{tr} < L \leqslant L_{\max}$, while maintaining symmetry and relative accuracy.

So, in augmented-KKR theory, we analytically evaluate Eq. (9) to include $L > L_{tr}$ (in the limit $\delta_l \to 0$) terms via linear algebra, rather than full matrix inversion. First, $g_{LL'}$ is calculated for $L \leqslant L_{\max}$ to where augmentation is desired. Second, for $L \leqslant L_{tr}$, the terms in Eq. (9) are evaluated as usual, while, for $L > L_{tr}$ in the $\delta_l \to 0$ limit, the first two terms can be analytically simplified using

$$\mathbf{Zt} \xrightarrow[\delta_l\to 0]{} +\mathbf{j}(\kappa r)$$
$$(\mathbf{ZtZ}-\mathbf{ZJ}) \xrightarrow[\delta_l\to 0]{} -\kappa\,\mathbf{j}(\kappa r)[i\,\mathbf{j}(\kappa r)-\mathbf{n}(\kappa r)]. \quad (10)$$

Equation (10) is derived rigorously (see the Appendix) using expressions for spherical potentials, which vanish outside of spheres inscribed within each cell. They do not hold for full-cell potentials, where nondiagonal L,L' terms can contribute generally, but can be derived.

Last, the most crucial step is evaluating the last term in Eq. (9). Positing negligible scattering for large L's, the last term is calculated in three steps:

(1) Calculate $\tau_{L_1L_2} = [(\mathbf{1}-\mathbf{tg})^{-1}\mathbf{t}]_{L_1L_2}$ for $L_i \leqslant L_{tr}$ by exact inversion.

(2) With $g_{LL'}$ ($\forall\, L,L' = L_{\max} > L_{tr}$), calculate $\mathbf{g}\tau\mathbf{g}$ using

$$(\mathbf{g}\tau\mathbf{g})_{LL'} = \sum_{L_1}^{L_{tr}}\sum_{L_2}^{L_{tr}}(g_{LL_1})(\tau_{L_1L_2})(g_{L_2L'}). \tag{11}$$

(3) Having $\mathbf{g}\tau\mathbf{g}$, multiply $(\mathbf{Zt})_{LL'}$ from both sides to get $\mathbf{G}(\mathbf{r},\mathbf{r}',E)$ for all $L = L_{\max}$.

With this, one needs to perform an inversion ($\mathcal{R}^3$ operation) only for matrices up to L_{tr}, and the higher-L contributions are included by matrix multiplication ($\mathbf{g}\tau\mathbf{g}$), which is computationally much faster ($\mathcal{R}^2$ operation).

For nonspherical potentials, one can derive expressions similar to Eq. (10) having off-diagonal (L,L') components. So, our three-step process to get the last term of Eq. (9) remains unchanged, except that $\mathbf{t}$ is nondiagonal. As such, the advantage of a rank-one update is lost when multiplying diagonal and off-diagonal matrices, i.e., $\mathbf{t}$ with $\mathbf{g}$ or $\mathbf{Zt}$ with $\mathbf{g}\tau\mathbf{g}$. Yet, the scaling for the multiple-scattering calculations remains unaltered. The solution of the nondiagonal components of the matrices, such as $\mathbf{t}$, are more rapidly calculated using the analytic diagonal solutions and iterating Dyson's equation until convergence, with integrations performed over convex Voronoi polyhedra, rather than spheres [29]. For full potentials involving arbitrarily shaped convex polyhedra, we have developed an efficient three-dimensional (3D) isoparametric method [30] to perform the integrations for solution of Schrödinger and Poisson's equations [31]. This method is more accurate and multiple orders of magnitude faster than conventional shape-function methods. Implementing the augmented-KKR formalism for full potentials is planned. Because the numerical effort of solving the multiple scattering is the same for both spherical and nonspherical potentials, the additional effort for the full-potential case in KKR theory scales linearly with the number of nonequivalent atoms.

In an all-electron, *ab initio* calculation for real systems, l truncation enters at several places and collectively affects, e.g., the cell DOS, and charge and magnetization densities. In turn, the Fermi energy E_{F} and magnetization M, defined from the sum rules

$$\mathrm{N(E_F)} = \int_{E_{\mathrm{bot}}}^{E_{\mathrm{F}}}[n_\uparrow(E') + n_\downarrow(E')]dE' = Z_{\mathrm{val}},$$
$$\mathrm{M} = \int_{E_{\mathrm{bot}}}^{E_{\mathrm{F}}}[n_\uparrow(E') - n_\downarrow(E')]dE', \tag{12}$$

are affected, as is the total energy. Here, E_{bot} designates the bottom of the valence band, $n_\uparrow(n_\downarrow)$ is the spin majority (minority) DOS, and Z_{val} is the average number of valence electrons. As will be shown, l truncation plays a significant role in correctly evaluating the E_{F} and M.

III. COMPUTATIONAL DETAILS

An all-electron, DFT KKR GF code [32] is used to perform the calculations, as previously done [4,7,8]. For the present results, the von Barth–Hedin [33] local spin-density approximation (LSDA), as parametrized by Moruzzi, Janak, and Williams [34], was used. The site-dependent Voronoi polyhedra were represented within an ASA sphere [35], with multicomponent cases handled by an optimal basis [24], where ASA spheres are adjust by saddle points in the electronic density. Complex energy contour integration with 24 energy points was used to integrate the Green's function. Monkhorst and Pack's [36] special $\mathbf{k}$-point method was used for Brillouin zone integration.

Following the above theory, distinct from conventional KKR theory, where L is truncated where $\delta_L(E) \approx 0$ (rather than where free-electron contributions are small, which is E, L, and temperature dependent), two distinct L_{tr} and $L_{\max}$ indices are used. All the calculations up to L_{tr} are performed in the standard way; i.e., for each energy E, we evaluate $(\mathbf{Z},\mathbf{J})$, $\mathbf{t}$, and $\mathbf{g}$ and get τ by inversion. For augmented-KKR theory, beyond L_{tr}, we calculate the truncated τ for $L,L' \leqslant L_{tr}$ and use the full $g_{LL'}$ matrix to augment $\mathbf{g}+\mathbf{g}\tau\mathbf{g}$ Eq. (11) up to $L_{\max}$, which can be chosen manually or to be below a specified tolerance for GF error. Recall from Eq. (9) that we know the analytic form of $\mathbf{ZtZ}-\mathbf{ZJ}$ and $\mathbf{Zt}$ for $L > L_{tr}$, so the only effort is in evaluating the matrix elements of $\mathbf{g}+\mathbf{g}\tau\mathbf{g}$ for $L_{tr} < L \leqslant L_{\max}$.

IV. RESULTS AND DISCUSSION

We apply the *ab initio* augmented-KKR formalism to fcc Cu, bcc Fe, and $\mathrm{L1_0}$ CoPt. The first two systems provide a stringent test of our formalism for a simple nonmagnetic and a magnetic system, respectively. The third illustrates application to a multisublattice, magnetic example.

A. Convergence of total energy and Fermi energy

Figure 1 shows the convergence of total energy (bottom) and Fermi energy (top) versus the augmentation $l_{\max}$, with $l_{tr} = 2,3,4$ for fcc Cu in our KKR ASA code [32]. The left-hand (right-hand) panel indicates the results for a basis of one Cu atom (atom + octahedral hole). The right-hand panel shows improvement in both augmentation and basis set, as the hole site makes the Voronoi polyhedra for each scattering site (atom and hole) more spherical, and the atom is better represented by an ASA sphere (and reduces the ASA overlap error), while the interstitial volume is greatly reduced.

The energies are not converged with $l_{tr} = 2$ and large $l_{\max}$ compared to converged values. By $l_{\max} = 5$ the total energy (E_{F}) reaches an asymptotic value, and the $l_{tr} = 2$ value is higher by 9 mRy (4 mRy) relative to those calculated with $l_{tr} = 4$. Beyond $l_{\max} = 5$, the error in total energy (E_{F}) is less than 0.05 mRy (0.01 mRy), i.e., the order of 1×10^{-5} Ry. For the one-atom Cu basis (left-hand panel), the total energy (E_{F}) with $l_{tr} = 4$ converged to within 1 mRy (0.1 mRy) compared to that with $l_{tr} = 3$. With an octahedral hole added to the basis (right-hand panel), the results are exactly the same for $l_{tr} = 3$ or 4. This is due to the use of a better basis set. As such, a faster convergence in the l space can be achieved by an improved basis set, but with a concomitant increase in the $\mathcal{R}^3$ process.

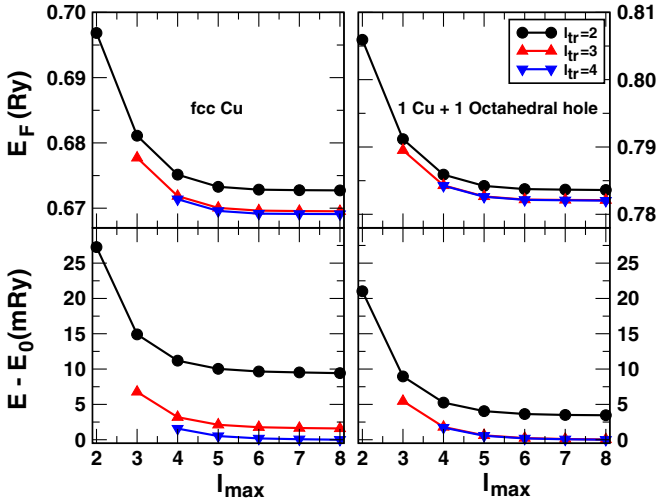

FIG. 1. (Color online) Left: Convergence properties of total energy E (bottom) and Fermi level E_F (top) vs l_{max} using different l_{tr} for one atom/cell fcc Cu. Right: Same as left, but for one Cu site plus one octahedral-hole site per cell. E_0 is defined by the $l_{tr} = 4, l_{max} = 8$ result. E_F is different on the left because of the Madelung potential inherent on the right.

Moghadam *et al.* [37] carried out a test of l convergence for fcc Cu in a real-space KKR, linear-scaling multiple-scattering (LSMS) method. The difference between the total energy (E_F) for $l_{max} = 3$ and $l_{max} = 8$ is 7 mRy (6 mRy). For the **k**-space-based, augmented-KKR theory, the differences are 6.5 mRy (8 mRy) for the one-Cu-site basis, and 5 mRy (7 mRy) for a basis with a Cu plus an octahedral hole. The present method, however, is computationally faster due to the augmentation used to evaluate the contribution of higher l's.

Figure 2 shows the convergence of total energy (bottom), E_F (middle), and magnetic moments (top) for magnetic bcc Fe (left-hand panel) and $L1_0$ CoPt (right-hand panel). As in the case of fcc Cu, the total energy and E_F converge by $l_{max} = 5$ with $l_{tr} = 4$. The converged moment of bcc Fe is $2.30\mu_B$, which compares well with the experimental value [38]

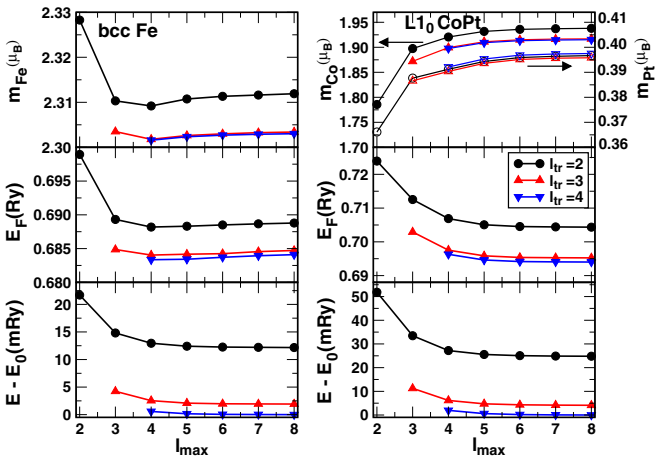

FIG. 2. (Color online) Convergence of total energy E (bottom), E_F (middle), and magnetic moments (top) vs l_{max} at different l_{tr} for a one-atom bcc Fe (left), and for a two-atom $L1_0$ CoPt (right). E_0 is an $L_{max} = 8$ reference value.

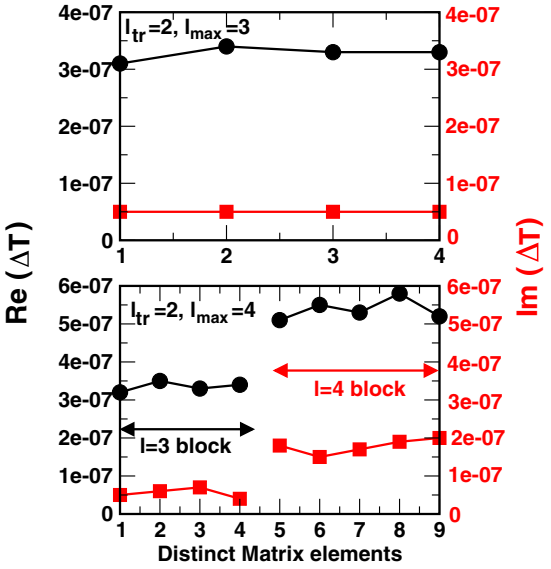

FIG. 3. (Color online) Absolute difference in distinct elements of $T_{LL'} = (g + g\tau g)_{LL'}$ calculated using full $\tau_{LL'}$ with $L, L' \leqslant L_{max}$ and the augmented-KKR $\tau_{LL'}$ with $L, L' \leqslant L_{tr} = 2$ and $L_{max} = 3$ (top) and $L_{max} = 4$ (bottom) at $E = (-0.76, 0.003)$ Ry. Similar accuracy is found along the entire semicircular contour of integration. For spherically symmetric scatterers with $L_{max} = 3$ (4), there are four (five) distinct matrix elements in the $L = 3$ (4) block of the T matrix.

of $2.2\mu_B$. The Co and Pt moment in $L1_0$ CoPt converges relatively slower compared to that of Fe. This is due to a slight c/a distortion in the $L1_0$ structure ($c/a = 0.984$). Calculated moments for Co and Pt are $1.91\mu_B$ and $0.396\mu_B$, respectively, compared to $1.76\mu_B$ and $0.35\mu_B$ from experiment at finite temperature [39].

Last, for comparison of matrix elements from full-KKR versus augmented-KKR theory, we first calculated τ for $L, L' \leqslant L_{max}$ by direct inversion, and then calculated the $\mathbf{T} = \mathbf{g} + \mathbf{g}\tau\mathbf{g}$ matrix using both full and truncated τ matrices. Figure 3 shows the absolute error (ΔT) in the matrix elements of the larger ($L > L_{tr}$) block of the augmented T-matrix calculated using full τ and truncated τ for fcc Cu. With $l_{tr} = 2$, the augmentation is compared for $l_{max} = 3$ ($l_{max} = 4$) in the top (bottom) panel. For fcc symmetry, there are four (five) distinct matrix elements in the $l = 3$ ($l = 4$) block of the T matrix, which are labeled along the horizontal axis. Clearly, augmented-KKR theory well reproduces the higher-l block of T matrices compared to full-KKR inversion (quite well below 1×10^{-6}), showing that the computationally faster augmentation has very good accuracy.

B. Comparison to Lloyd's formula

Lloyd's formula is the N-site generalization of the Friedel (single-site) sum rule, or optical theorem, for the electronic integrated DOS:

$$N(E) = N_{\text{free}}(E) + \frac{2}{\pi}\sum_{\ell}(2\ell + 1)\delta_\ell(E), \qquad (13)$$

where $N_{\text{free}}(E)$ is the integrated DOS of the free electrons, known analytically in three dimensions, i.e., $E^{3/2}/(6\pi^2)$. [For

complex E, Eq. (13) is incorrect but can be generalized via scattering matrices.] The KKR Lloyd's formula for an ordered system can be written in spectral representation at any complex E as [40–42]

$$N(E) = N_{\rm free}(E) + \frac{1}{\pi}{\rm Im}\ln||\alpha(E)|| - \frac{1}{N_k}\Sigma_{\mathbf{k}}\frac{1}{\pi}{\rm Im}\ln||1-\mathbf{t}(E)\mathbf{g}(\mathbf{k},E)|| \qquad (14)$$

for discrete samples in $\mathbf{k}$ space, with $\alpha(E)$ defined by the scattering solutions of $v(r)$ near the scattering centers. The determinant is performed over both basis-site and angular-momentum indices, and it is equivalent to an eigenvalue sum, albeit done by constant-E scan. The formula is also related to Krein's theorem [43,44]. Lloyd's formula is an amazing result being the closed-form expression for the integrated DOS at any E (total electrons)! Moreover, a variation of Lloyd's formula with respect to potential $v(\mathbf{r})$ yields the density at any energy $\rho(\mathbf{r};E)$ to second order in changes in the self-consistent potential (e.g., higher-order L's) and, hence, in $E_{\rm F}$ [4].

Because the KKR determinant passes through zero at every Bloch solution, it picks up a phase of π at these locations, giving the number of electrons up to E. Equation (14) counts jumps in phases in the KKR determinant ("Im log" operation). There is a practical implementation issue: *At a given E* the phase is known to modulo 2π (or total electrons within a whole number), but trivially handled with a good $E_{\rm F}$ estimate from the real-space GF. Thus, Lloyd's formula gives an exact (no L truncation) $E_{\rm F}$ and electron count from a few values of E.

Importantly, here, the augmented-KKR formulation is expected to yield a value of $E_{\rm F}$ consistent with that obtained by Lloyd's formula. Also, for thermodynamics of a system, an analytic expression for the free-energy functional can be directly derived from Lloyd's formula using a Gibbs relation [4], which we use to calculate the total (free) energy. At finite temperature it directly yields Mermin's theorem, or the Kohn-Sham theorem at 0 K [4]. Hence, the spectral Lloyd's formula specifies the thermodynamics and correct Fermi surface at $E_{\rm F}$.

To assess the augmented-KKR $E_{\rm F}$ and electron count, we must compare three results: (1) convergence of the augmented-KKR spectral GF—Lloyd's formula; (2) convergence of the augmented-KKR real-space GF, as given by the trace of Eq. (9); and (3) convergence of items 1 and 2 with improved basis. Notably, approach 2 is used in a typical self-consistent-field (SCF) KKR GF for computational expediency because $\mathbf{G}(\mathbf{r},\mathbf{r}';E)$ is always handy.

To be clear, results 1 and 2 should agree for an exact method. However, these values will differ if there is any approximation that is not handled equivalently in k space and real space, as in the ASA. For result 1 above, $\mathbf{G}(\mathbf{r},\mathbf{r}';E)$ is evaluated within an ASA sphere and then Fourier transformed to obtain $\mathbf{G}(\mathbf{k};E)$ commensurate with the Brillouin zone of the full unit cell; hence, for ordered systems, it is a calculation of the volume enclosed by the Fermi surface and corresponds to the count over a *nonspherical* charge distribution. In contrast, for result 2, the trace of $\mathbf{G}(\mathbf{r},\mathbf{r}';E)$ is evaluated in an ASA sphere, which does not account for the volume as done in result 1, and it must suffer a modest error because only a spherical charge density is considered. Therefore, result 1 above should be correct, and a small error may appear from result 2, which will decrease with, say, improving basis.

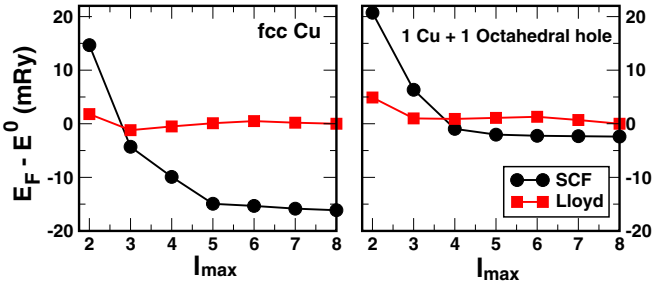

FIG. 4. (Color online) $E_{\rm F}$ by real-space GF (circle) relative to spectral Lloyd's formula (square) for Cu (left) and Cu plus hole (right) for $L_{tr} = L_{\rm max}$. E^0 is a reference energy.

For comparison, a wave-function approach using the ASA solves the secular equation after Fourier transform by diagonalization to get the eigenvalues, and $E_{\rm F}$ is then obtained by counting states within the volume enclosed by the Fermi surface; then the remaining quantities are determined by referencing only k space. As such, it is equivalent to the value from the spectral Lloyd's formula, Eq. (14).

From the SCF KKR approach, Fig. 4 compares $E_{\rm F}$ versus $L_{\rm max}$ $(=L_{tr})$ from a real-space Green's function (circle) and from a spectral (k-space) Lloyd's formula (square) for basis with one Cu (left) and for one Cu plus an octahedral hole (right). These results agrees with those from the augmented-KKR approach with $L_{tr} = 3$ but evaluated for each $L_{\rm max} \leqslant 8$. As is apparent, the spectral Lloyd's results converge rapidly, whereas those from real space converge slower and suffer a small error because only a spherical charge density is considered. As is obvious from Fig. 4, the discrepancy in $E_{\rm F}$ obtained from the two methods reduces when an octahedral hole is inserted into the fcc cell (right-hand panel) because the ASA then better represents the real-space volume; the k-space result is also improved because the nonspherical charge density is better represented.

As discussed elsewhere (e.g., for applications to warm-dense matter), further improvements to the agreement between real-space and k-space results (not shown) are possible, which leads to much less than 1 mRy discrepancy. Example changes include improving the normalization of scattering functions (**Z, J**), and including $N_{\rm free}(E)$ analytically (infinite L sum), as in Lloyd's formula, while simultaneously removing the L-truncated free-electron Green's function contributions from the KKR Green's function during the SCF cycle.

C. Convergence of structural parameters

Up to now we have investigated the convergence properties at a fixed lattice parameter. Another important thing to check is how convergence affects the accuracy of the equilibrium (ground-state) lattice parameter. Figure 5 shows the energy versus lattice constant (a) for fcc Cu (top) and bcc Fe (bottom) at different sets of l truncation. Notably, for both systems, the energy curve with $l_{tr} = 4$ and $l_{\rm max} = 6$ is almost indistinguishable

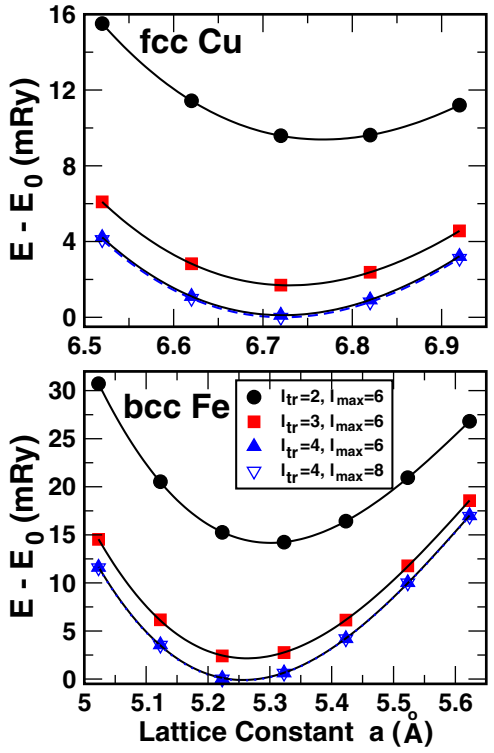

FIG. 5. (Color online) Total energy vs a for various sets of augmentation $(L_{tr}, L_{\max})$ for Cu (top) and Fe (bottom).

from that with $l_{\max} = 8$, indicating the convergence by $l_{\max} = 6$. Already $l_{tr} = 3$ finds a similar minimum to that from larger l_{tr}; however, $l_{tr} = 2$ is not a reliable choice for converged results. The calculated 0 K lattice constants for fcc Cu and bcc Fe are 6.72 and 5.26 a.u., respectively, which compare well with room-temperature experimental values (6.82 and 5.42 a.u., respectively) and previous LSDA results.

D. Estimate of numerical savings

In the current implementation the augmented-KKR approach requires $[N^3(l_{tr}+1)^3 + N^2(l_{\max+1}+1)(l_{tr}+1)]$ operations compared to $[N(l_{\max}+1)]^3$ operations in the standard KKR approach. For reliable convergence in the present examples, we found $l_{tr} = 3$ and $l_{\max} = 8$ to be sufficient for lattice constants and structural energy differences, in which case we require $(64N^3 + 36N^2)$ operations as opposed to $278N^3$ operations. Hence, about three- to fourfold less computational time is required for cells with 1–10 atoms—an estimate that holds the calculations done here.

V. CONCLUSION

Motivated by physics and resulting numerical efficiency, we have presented and implemented an augment-KKR Green's function formalism that accurately handles multiple scattering (where phase shifts are not zero) by direct inversion of a smaller L_{tr}-truncated basis and includes higher $L > L_{tr}$ by linear algebra for necessary single-site and free-electron contributions. We applied the augmented-KKR formalism to three systems and showed very good convergence properties and accuracy compared to KKR with direct inversion to $L_{\max}$, although we discovered that a larger L basis is needed over that generally assumed. To be mathematically consistent, the L-sum truncations for wave functions and scattering matrices need to be done in tandem with each other [see Eq. (9)] due to a normalization factor occurring in both the single-site wave functions and $\mathbf{t}$ matrices. By identifying this common normalization, one can analytically evaluate the $\delta_l \to 0$ limit to include higher L's via simple linear algebra, instead of the exact inversion as required in the conventional KKR approach, saving significant computational effort while improving accuracy. For nonspherical potentials, one can derive the expressions with $\mathbf{t}$'s no longer diagonal, but the approach and the scaling for the multiple-scattering calculations remains unchanged. The augmented-KKR approach can be extended to the coherent potential approximation (CPA) and dynamical cluster approximation (DCA) to handle disorder, as will be presented elsewhere.

ACKNOWLEDGMENTS

A.A. acknowledges support from SEED Grant (sponsored Project No. 13IRCCSG020) at IIT Bombay. Work was supported by the U.S. Department of Energy, Office of Science, Basic Energy Sciences, Materials Science and Engineering Division, partially through the Center for Defect Physics, an Energy Frontier Research Center (A.A., D.M.N., and S.N.K. for Ph.D. thesis), and through Ames Laboratory under Contract No. DE-AC02-07CH11358 for materials discovery (A.S., D.D.J., and S.N.K. for post-doc), and Contract No. DE-FG02-03ER46026 for supplemental code (A.S. and D.D.J.). The research was performed at Ames Laboratory, operated for the U.S. Department of Energy by Iowa State University under Contract No. DE-AC02-07CH11358.

APPENDIX: DERIVATION OF EQ. (10)

To derive Eq. (10), consider the matrix representation of Eqs. (2), (4), (5), and (7). In the limit $\delta_l \to 0$, the sine and cosine matrices $\mathbf{S}$ and $\mathbf{C}$ go to, respectively, zero and unitary matrix, where $|\mathbf{C}| \sim |e^{i\phi}| = 1$. Then, accounting for cancellations of sine matrices in the numerator and denominator, we find

$$\mathbf{Zt} = -(\mathbf{nS} - \mathbf{jC})e^{+i\delta_l} \underset{\delta_l \to 0}{\longrightarrow} \mathbf{j}(\kappa r). \tag{A1}$$

Similarly,

$$\mathbf{ZtZ} = -\kappa \frac{(\mathbf{nS} - \mathbf{jC})(\mathbf{nS} - \mathbf{jC})e^{+i\delta_l}}{\mathbf{S}},$$

$$\mathbf{ZJ} = \kappa \frac{(\mathbf{nS} - \mathbf{jC})\mathbf{j}}{\mathbf{S}}.$$

As $\delta_l \to 0$, and we apply limit evaluation rules, we find

$$\mathbf{ZtZ} \underset{\delta_l \to 0}{\longrightarrow} -\kappa\,[i\,\mathbf{j}(\kappa r)\,\mathbf{j}(\kappa r) - 2\,\mathbf{j}(\kappa r)\,\mathbf{n}(\kappa r)],$$

$$\mathbf{ZJ} \underset{\delta_l \to 0}{\longrightarrow} +\kappa\,\mathbf{j}(\kappa r)\,\mathbf{n}(\kappa r).$$

Therefore,

$$\mathbf{ZtZ} - \mathbf{ZJ} \underset{\delta_l \to 0}{\longrightarrow} -\kappa\,\mathbf{j}(\kappa r)[i\,\mathbf{j}(\kappa r) - \mathbf{n}(\kappa r)]. \tag{A2}$$

[1] J. Korringa, Physica (Utrecht) **13**, 392 (1947).
[2] W. Kohn and N. Rostoker, Phys. Rev. **94**, 1111 (1954).
[3] H. Ebert, D. Ködderitzsch, and J. Minár, Rep. Prog. Phys. **74**, 096501 (2011), and references therein.
[4] D. D. Johnson, D. M. Nicholson, F. J. Pinski, B. L. Gyorffy, and G. M. Stocks, Phys. Rev. Lett. **56**, 2088 (1986); Phys. Rev. B **41**, 9701 (1990).
[5] D. D. Johnson, A. V. Smirnov, J. B. Staunton, F. J. Pinski, and W. A. Shelton, Phys. Rev. B **62**, R11917(R) (2000).
[6] A. V. Smirnov, W. A. Shelton, and D. D. Johnson, Phys. Rev. B **71**, 064408 (2005).
[7] Aftab Alam and D. D. Johnson, Phys. Rev. B **85**, 144202 (2012).
[8] Aftab Alam, Brent Kraczek, and D. D. Johnson, Phys. Rev. B **82**, 024435 (2010).
[9] W. H. Butler, X-G. Zhang, T. C. Schulthess, and J. M. MacLaren, Phys. Rev. B **63**, 054416 (2001).
[10] Aftab Alam and D. D. Johnson, Phys. Rev. Lett. **107**, 206401 (2011).
[11] W. H. Butler and G. M. Stocks, Phys. Rev. B **29**, 4217 (1984); G. M. Stocks and W. H. Butler, Phys. Rev. Lett. **48**, 55 (1982).
[12] *Application of Multiple Scattering Theory to Materials Science: Symposium Held December 2-5, 1991, Boston, Massachusetts, USA*, edited by W. H. Butler *et al.* (Materials Research Society, Pittsburgh, PA, 1992), Vol. 253.
[13] J. B. Pendry, *Low Energy Electron Diffraction* (Academic, London, 1974).
[14] M. A. Van Hove, *Low Energy Electron Diffraction: Experiment, Theory and Surface Structure Determination* (Springer-Verlag, New York, 1986).
[15] P. J. Durham, R. G. Jordan, G. S. Sohal, and L. T. Wille, Phys. Rev. Lett **53**, 2038 (1984); see also P. J. Durham, J. Phys. F: Met. Phys. **11**, 2475 (1981).
[16] J. E. Inglesfield, Rep. Prog. Phys. **45**, 223 (1982); H. Ebert, *ibid.* **59**, 1665 (1996).
[17] J. Braun, J. Minár, S. Mankovsky, V. N. Strocov, N. B. Brookes, L. Plucinski, C. M. Schneider, C. S. Fadley, and H. Ebert, Phys. Rev. B **88**, 205409 (2013).
[18] J. B. Staunton, D. D. Johnson, and F. J. Pinski, Phys. Rev. Lett. **65**, 1259 (1990).
[19] J. D. Althoff, D. D. Johnson, and F. J. Pinski, Phys. Rev. Lett. **74**, 138 (1995); J. D. Althoff, D. D. Johnson, F. J. Pinski, and J. B. Staunton, Phys. Rev. B **53**, 10610 (1996).
[20] J. B. Staunton, J. Poulter, B. Ginatempo, E. Bruno, and D. D. Johnson, Phys. Rev. Lett. **82**, 3340 (1999).
[21] W. H. Butler, Phys. Rev. B **41**, 2684 (1990).
[22] X.-G. Zhang and W. H. Butler, Phys. Rev. B **46**, 7433 (1992).
[23] B. L. Györffy and M. J. Stott, Solid State Commun. **9**, 613 (1971).
[24] Aftab Alam and D. D. Johnson, Phys. Rev. B **80**, 125123 (2009); also, derivation by D. D. Johnson (unpublished).
[25] Albert Messiah, *Quantum Mechanics*, Vol. 1 (Wiley, New York, 1966), Chaps. IX and X.
[26] D. D. Johnson, F. J. Pinski, and G. M. Stocks, Phys. Rev. B **30**, 5508 (1984).
[27] Duane D. Johnson, Ph.D. thesis, University of Cincinnati, 1985.
[28] F. J. Pinski and G. M. Stocks, Phys. Rev. B **32**, 4204 (1985).
[29] N. Papnikolau, R. Zeller, and P. H. Dederichs, J. Phys.: Condens. Matter **14**, 2799 (2002).
[30] Aftab Alam, S. N. Khan, B. G. Wilson, and D. D. Johnson, Phys. Rev. B **84**, 045105 (2011).
[31] Aftab Alam, B. G. Wilson, and D. D. Johnson, Phys. Rev. B **84**, 205106 (2011).
[32] D. D. Johnson and A. Alam, *MECCA: Multiple-scattering Electronic-structure Calculations for Complex Alloys (KKR-CPA Program, ver. 2.0)* (University of Illinois, Urbana-Champaign, IL, 2008).
[33] U. Von Barth and L. Hedin, J. Phys. C: Solid State Phys. **5**, 1629 (1972).
[34] V. L. Moruzzi, J. F. Janak, and A. R. Williams, *Calculated Electronic Properties of Materials* (Pergamon, New York, 1978).
[35] P. Phariseau and W. M. Temmerman, *The Electronic Structure of Complex Systems* (Plenum, New York, 1984).
[36] H. J. Monkhorst and J. D. Pack, Phys. Rev. B **13**, 5188 (1976).
[37] N. Y. Moghadam, G. M. Stocks, X.-G. Zhang, D. M. C. Nicholson, W. A. Shelton, Yang Wang, and J. S. Faulkner, J. Phys.: Condens. Matter **13**, 3073 (2001).
[38] Mathias Ekman, Babak Sadigh, Kristin Einarsdotter, and Peter Blaha, Phys. Rev. B **58**, 5296 (1998).
[39] W. Grange, I. Galanakis, M. Alouani, M. Maret, J.-P. Kappler, and A. Rogalev, Phys. Rev. B **62**, 1157 (2000).
[40] P. Lloyd, Proc. Phys. Soc. London **90**, 207 (1967).
[41] P. Lloyd and P. V. Smith, Adv. Phys. **21**, 69 (1972).
[42] Rudolf Zeller, J. Phys.: Condens. Matter **16**, 6453 (2004).
[43] M. G. Krein, Mat. Sb. **33**, 597 (1953).
[44] J. S. Faulkner, J. Phys. C: Solid State Phys. **10**, 4661 (1977).